Introduction to structural health monitoring with piezoelectric wafer active sensors

V. GIURGIUTIU

University of South Carolina, Department of Mechanical Engineering, Columbia, USA
E-mail: victorg@sc.edu

Key Words

Structural health monitoring, SHM, nondestructive evaluation, NDE, piezoelectric wafer active sensors, PWAS, power, energy; embedded ultrasonics structural radar, EUSR, crack detection, crack growth, damage detection

1. Introduction

Structural health monitoring (SHM) uses a set of permanently attached sensors to obtain on demand information about the structural performance and its 'health state' [1]. The benefits of monitoring the structural state include design feedback, performance enhancement, on-demand condition-based maintenance, and predictive fleet-level prognosis. On-board structural sensing systems have been envisioned for determining the health of a structure by monitoring a set of sensors over time, assessing the remaining useful life from the recorded data and design information, and advising of the need for structural maintenance actions. Piezoelectric wafer active sensors (PWAS) have emerged as one of the major SHM technologies; the same sensor installation can be used with a variety of damage detection methods: propagating ultrasonic guided waves, standing waves (E/M impedance) and phased arrays. Structural health monitoring (SHM) is a multidisciplinary process involving several disciplines that must be closely coordinated (Figure 1).

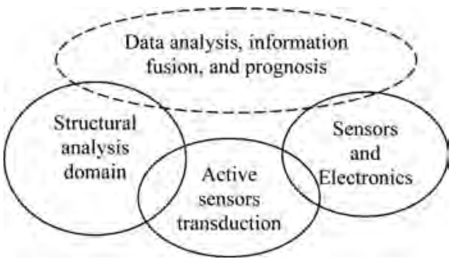

Figure 1. Venn diagram of the multi-domain interaction during structural sensing.

Guided-waves techniques for nondestructive evaluation (NDE) and structural health monitoring (SHM) applications are increasingly popular due to their ability to cover large areas with a relatively small number of sensors [2]. Miniaturized guided-wave transducers, such as piezoelectric wafers attached directly to structural elements, have gained large popularity due to their low cost, simplicity, and versatility [3]. These transducers can actively interrogate the structure using a variety of guided-wave methods such as pitch-catch, pulse-echo, phased arrays, and electromechanical (E/M) impedance technique. The can be also used passively for impact detection or acoustic emission (AE). These transducers can be developed into ultra-lightweight integrated ferroelectric thin films that may be manufactured directly on the structural materials through nano-fabrication techniques [4].

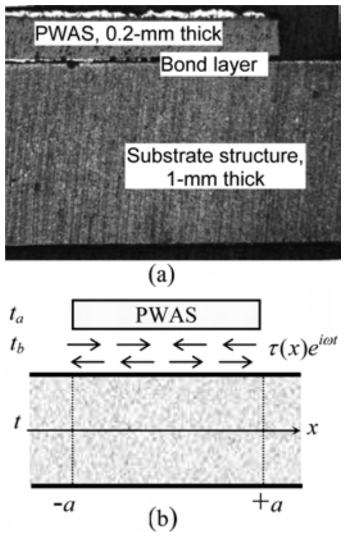

Figure 2. Bond-layer between PWAS and structure: (a) micrograph; (b) modeling [5].

An onboard SHM system could contain (a) sensors and sensor clusters; (b) electronics; (c) data processing and communications. The sensors can be either **passive** (strain, temperature, acceleration, etc.) or **active** (e.g., ultrasonic transducers that can interrogate the structure to detect damage presence, extent, and intensity). Passive structural sensing has been used to gather historical data about fleet usage and structural loads. Active structural sensing NDE techniques have been used to inspect the structure during maintenance actions, which are far apart and labor intensive. **The desire exists for onboard active sensing systems that would interrogate the structure at will and produce on-demand structural health bulletins.** The challenge in developing such active sensing systems is to develop integrated miniaturize transducers that can be permanently bonded to the structure and left in place to be activated on demand.

2. Piezoelectric wafer active sensors

Piezoelectric wafer active sensors (PWAS) couple the electrical and mechanical effects (mechanical strain, S_{ij}, mechanical stress, T_{kl}, electrical field, E_k, and electrical displacement, D_j) through the tensorial piezoelectric constitutive equations

$$\begin{aligned} S_{ij} &= s^E_{ijkl} T_{kl} + d_{kij} E_k \\ D_j &= d_{jkl} T_{kl} + \varepsilon^T_{jk} E_k \end{aligned} \qquad (1)$$

where, s^E_{ijkl} is the mechanical compliance of the material measured at zero electric field (E=0), ε^T_{jk} is the dielectric permittivity measured at zero mechanical stress (T=0), and d_{kij} represents the piezoelectric coupling effect. PWAS utilize the d_{31} coupling between in-plane strains, S_1, S_2, and transverse electric field, E_3. PWAS are transducers are different from conventional ultrasonic transducers because [5]:

1. PWAS are firmly coupled with the structure through an adhesive bonding (Figure 2), whereas conventional ultrasonic transducers are weakly coupled through gel, water, or air.

2. PWAS are non-resonant devices that can be tuned selectively into several guided-wave modes, whereas conventional ultrasonic transducers are single-resonance devices.

3. Because PWAS are small, lightweight, and inexpensive they can be deployed in large quantities on the structure, which is not practical with conventional ultrasonic transducers, which are relatively bulky and expensive.

By using Lamb waves in a thin-wall structure, one can detect structural anomaly, i.e., cracks, corrosions, delaminations, and other damage.

PWAS transducers act as both transmitters and receivers of Lamb waves traveling through the structure. Upon excitation with an electric signal, the PWAS transmitter generates Lamb waves in a thin-wall structure. The generated Lamb waves travel through the structure and are reflected or diffracted by the structural boundaries, discontinuities, and damage. The reflected or diffracted waves arrive at the PWAS receiver where they are transformed into electric signals.

PWAS transducers can serve several purposes [5]: (a) high-bandwidth strain sensors; (b) high-bandwidth wave exciters and receivers; (c) resonators; (d) embedded modal sensors with the electromechanical (E/M) impedance method. By application types, PWAS transducers can be used for (i) active sensing of far-field damage using pulse-echo, pitch-catch, and phased-array methods, (ii) active sensing of near-field damage using high-frequency E/M impedance method and thickness-gage mode, and (iii) passive sensing of damage-generating events through detection of low-velocity impacts and acoustic emission at the tip of advancing cracks (Figure 3). The main advantage of PWAS over conventional ultrasonic probes is in their small size, lightweight, low profile, and small cost. In spite of their small size, PWAS are able to replicate many of the functions performed by conventional ultrasonic probes. Laboratory for active materials and smart structures (LAMSS) at the University of South Carolina, USA, has accumulated extensive experience in several active sensing methods using guided waves and PWAS transducers, as illustrated next.

3. Tuning of pwas to structural guided Lamb waves

The in-plane interaction between the PWAS and the guided Lamb waves is such that preferential tuning can be achieved when the representative PWAS dimensions are near an odd multiple of the half wavelength of certain Lamb-wave mode. Thus, selective tuning of various Lamb-wave modes can be achieved by setting the PWAS dimension to be the appropriate multiple of the half wavelength [6]. Giurgiutiu [6] developed the theory of the interaction of a rectangular PWAS with one-dimensional propagation, i.e., straight-crested Lamb waves, and presented tuning prediction formulae based on trigonometric functions.

$$\varepsilon_x(x,t)\big|_{y=d} = -i\frac{a\tau_0}{\mu}\left[\sum_{\xi^S}\sin(\xi^S a)\frac{N_S(\xi^S)}{D_S'(\xi^S)}e^{i(\xi^S x-\omega t)} + \sum_{\xi^A}\sin(\xi^A a)\frac{N_A(\xi^A)}{D_A'(\xi^A)}e^{i(\xi^A x-\omega t)}\right] \qquad (2)$$

Raghavan and Cesnik [7] extended these results to the case of a circular transducer coupled with circular-crested Lamb waves and proposed corresponding tuning prediction formulae based on Bessel functions:

$$\varepsilon_r(r,t)\big|_{z=d} = \pi\frac{\tau_0 a}{\mu}e^{i\omega t}\left[\sum_{\xi^S}J_1(\xi^S a)\xi^S\frac{N_S(\xi^S)}{D_S'(\xi^S)}H_1^{(2)}\left(\xi^S r\right) + \sum_{\xi^A}J_1(\xi^A a)\xi^A\frac{N_A(\xi^A)}{D_A'(\xi^A)}H_1^{(2)}\left(\xi^A r\right)\right] \qquad (3)$$

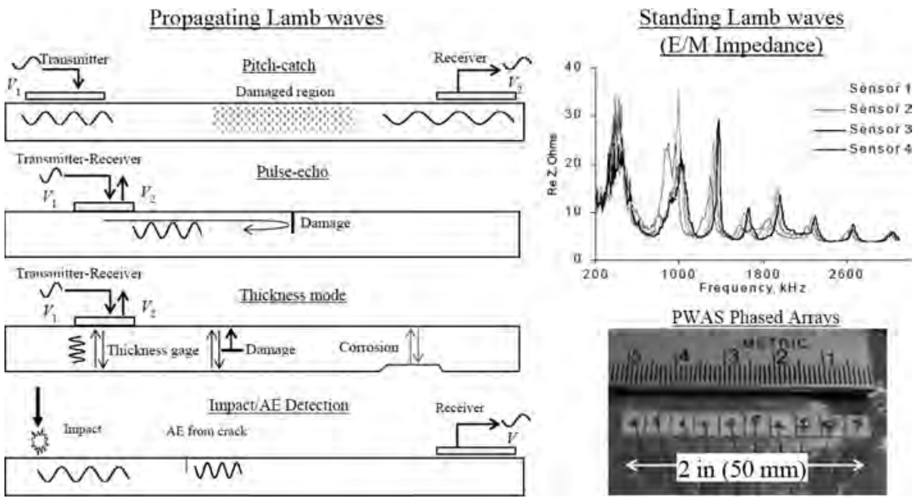

Figure 3. PWAS used for structural sensing include propagating Lamb waves, standing Lamb waves (electromechanical impedance) and phased arrays [5],

Figure 4 compares experimental and theoretical results for a 7-mm square PWAS placed on 1.07-mm 2024-T3 aluminum alloy plate. The experimental results (Figure 4a) show that a rejection of the highly dispersive A0 Lamb wave mode is observed at around 200 kHz. At this frequency, only the S0 mode is excited, which is very beneficial for pulse-echo studies due to the low dispersion of the S0 mode at this relatively low value of the *fd* product. On the other hand, a strong excitation of the A0 mode is observed at around 50 kHz. These experimental results were reproduced using Equation with the assumption that the effective PWAS length is 6.4 mm (Figure 4b). The difference between the actual PWAS length and effective PWAS length is attributed to shear transfer/diffusion effects at the PWAS boundary.

4. Direct structural imaging with EUSR-PWAS phased-arrays

By using Lamb waves in a thin-wall structure, one can detect the existence and positions of cracks, corrosions, delaminations, and other damage [8]. PWAS transducers act as both transmitters and receivers of Lamb waves traveling in the plate. Upon excitation with an electric signal, the PWAS generate Lamb waves into a thin-wall structure. The generated Lamb waves travel into the structure and are reflected or diffracted by the structural boundaries, discontinuities, and damage. The reflected or diffracted waves arrive back at the PWAS where they are transformed into electric signals.

Of particular interest is the phased-array implementation of this concept. The embedded ultrasonic structural radar (EUSR) is a phase-array application of the PWAS technology. The EUSR principles and initial results were reported extensively by Giurgiutiu and Bao [9].

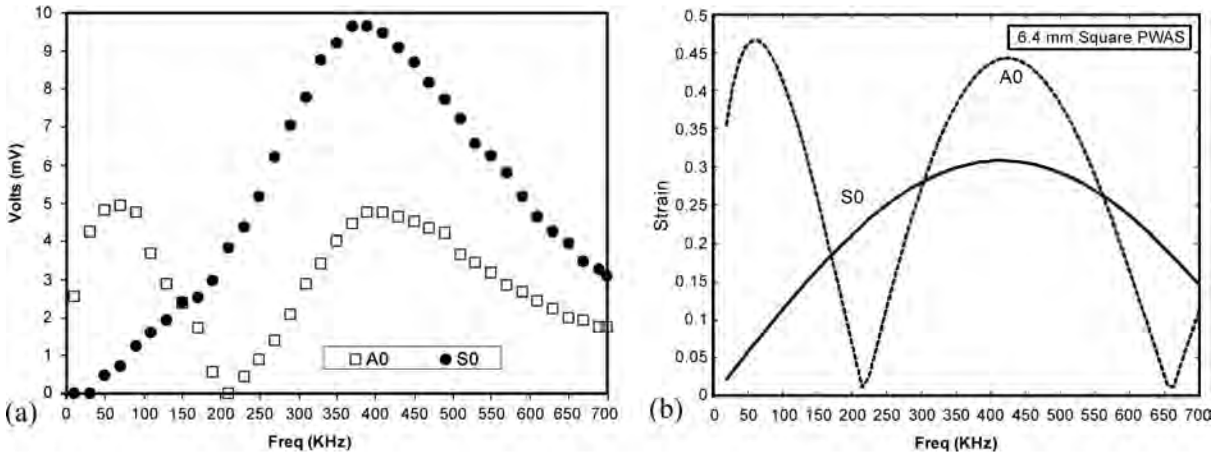

Figure 4. Lamb-wave tuning using a 7-mm square PWAS placed on 1.07-mm 2024-T3 aluminum alloy plate: (a) experimental results; (b) prediction with Equation for 6.4 mm effective PWAS length [5].

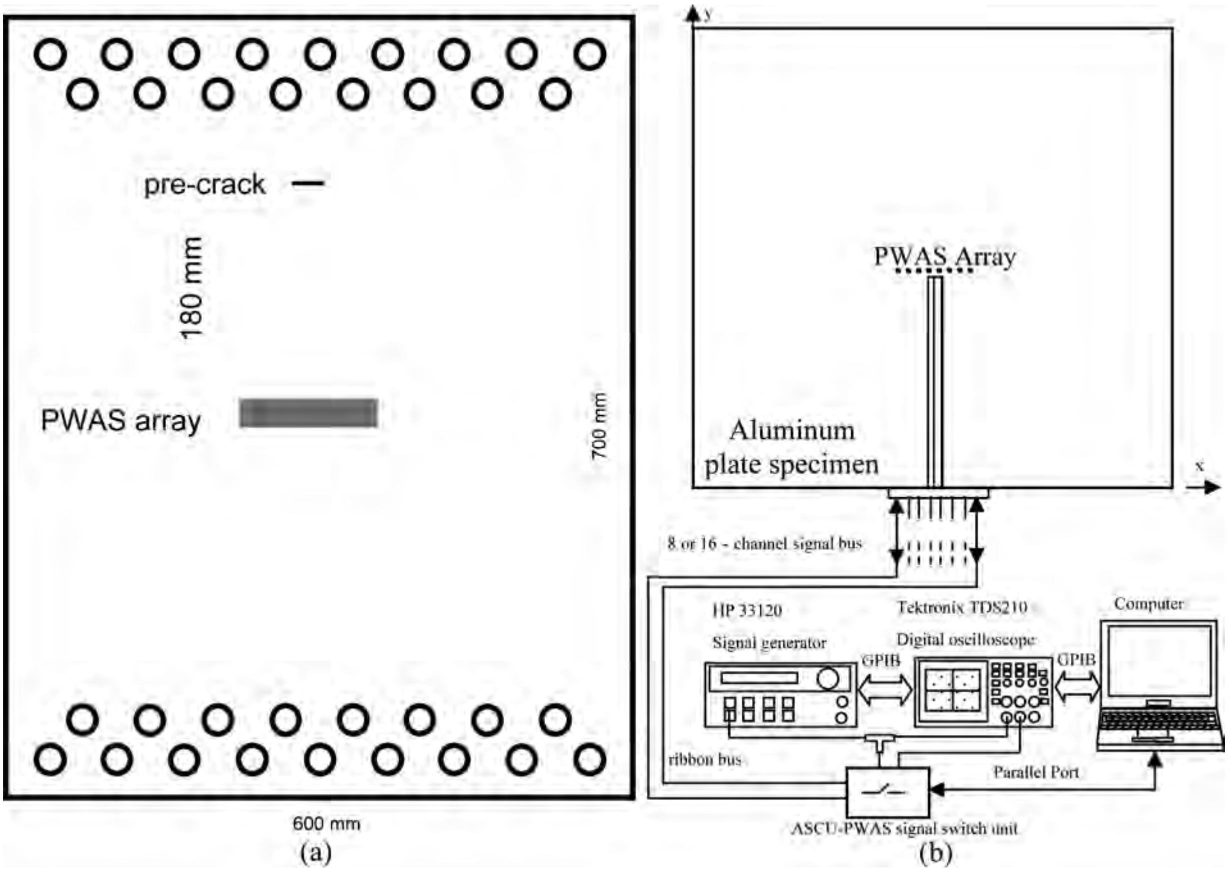

Figure 5. Schematic of experimental setup for fatigue testing with PWAS: (a) schematic of specimen #2 showing the installation of the PWAS array and the location of the precrack; (b) instrumentation schematics [10],

The basic idea of the EUSR algorithm is to use a group of PWAS arranged in a certain pattern and manipulate the synthetic output beam at a particular direction by adjusting the delays between the firing of each element. Among the possible array configurations, the linear array obtained by arranging elements along a straight line presents is the simplest one, as illustrated in Figure 5.

Sudarea şi Încercarea Materialelor

A 600-mm by 700-mm panel of 1-mm 2024-T3 aluminum alloy was instrumented [10] with a 10-PWAS phased array placed at its center (Figure 6). The instrumentation consisted of an HP 33120 signal generator, a TDS210 digital oscilloscope, an

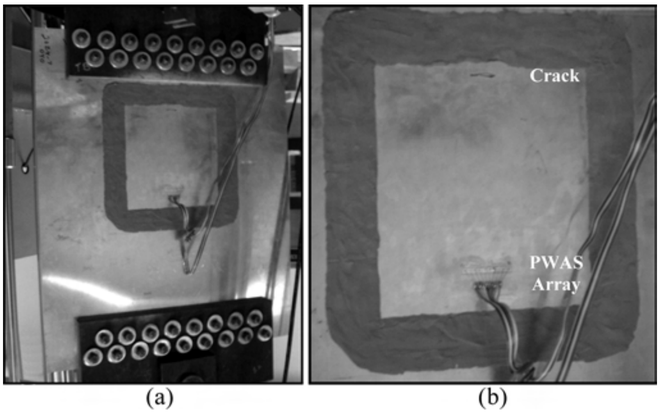

Figure 6. Experimental setup for fatigue testing with PWAS: (a) overall picture showing the specimen #2; (b) detail of the specimen showing the PWAS array, the crack, and the clay dam. [10].

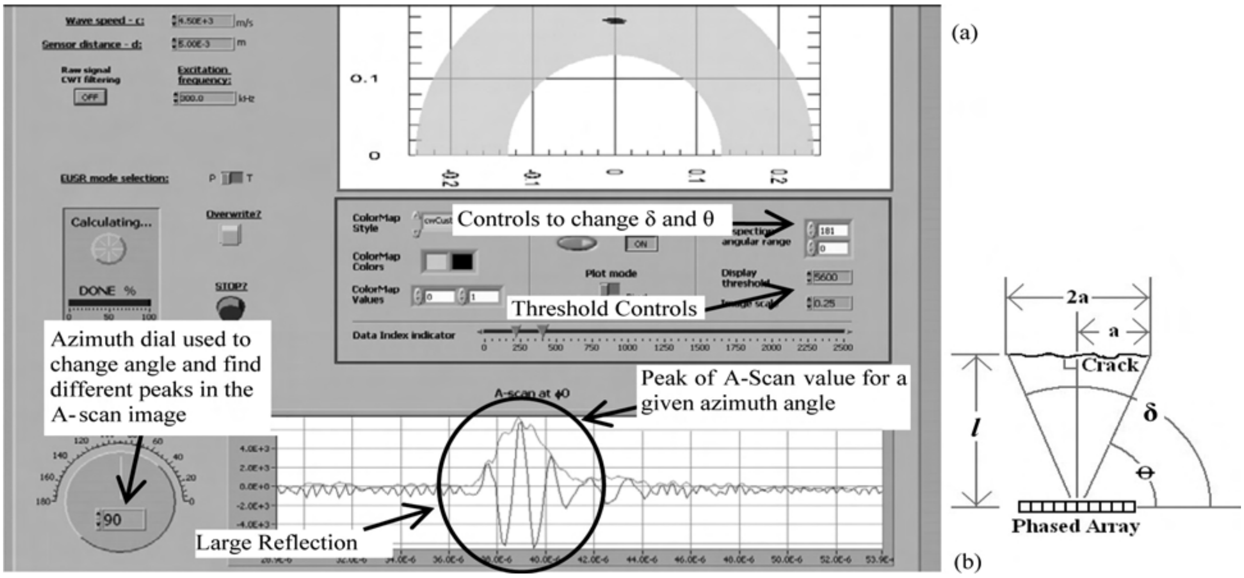

Figure 7. Determination of crack size from the GUI of the PWAS EUSR program: (a) annotated screen capture showing the angles and threshold controls of EUSR GUI; (b) schematic indicating the θ and δ angles in relation to the crack length, 2*a* and distance to the target [10].

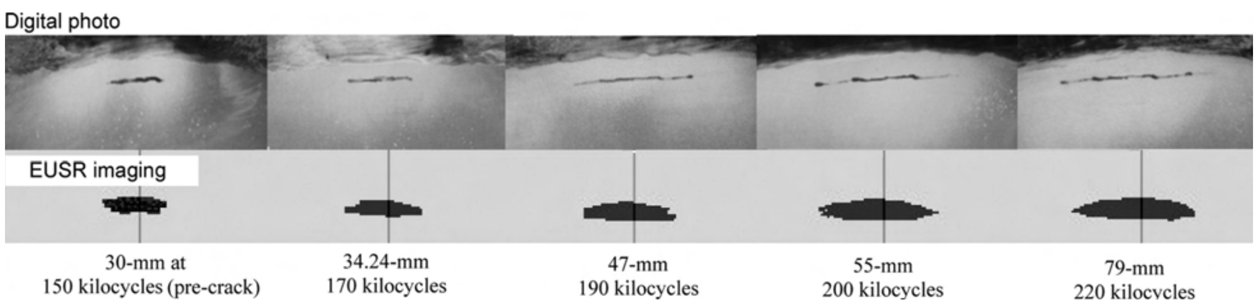

Figure 8. Comparison between images taken optically and scanned images using EUSR. Note photos have been adjusted for illustration. The illustrated crack lengths are measured optically in mm at various cycle counts in kilocycles [10].

ASCU auto-switch unit, and a laptop computer. The round-robin data collection is performed in the following way: a 3-count 372 kHz tone-burst excitation signal is synthesized in the function generator. At this frequency, the tone-burst signal obtained the optimum tuning of the PWAS with the S0 Lamb-wave mode being excited. The tone-burst signal is sent to one PWAS in the array, travels into the plate, and is reflected at the crack and later at the plate boundary. The reflected Lamb-waves packet is received back at the PWAS array.

The signals received at each PWAS in the array (including the transmitting PWAS) are collected by the DAQ device, i.e., the digital oscilloscope. This procedure is repeated for all the PWAS; generates a column of 10 elemental signals in the 100 elemental-signals array. After this, the cycle is repeated for the other PWAS in the round-robin fashion. For the 10-PWAS array, there will be 10 such measurement cycles necessary to complete the whole data collection process [10].

The EUSR algorithm software tool processes the measured PWAS phased array data at each cycle and produces an image of the scanning results. The EUSR image was then used to obtain an estimation of the crack size. Figure 7a shows the EUSR front panel. The threshold value, the values δ, and θ of the "dial angles" were controlled from the panel (Figure 7b). First, an approximate position of the crack edge is obtained with the azimuth dial. If the azimuth dial is turned to an angle where the synthetic beam find a target and gets a reflection, then the A-scan image will show a reflection echo as illustrated in

Figure 7a. After a threshold value was chosen, the θ and δ angles were adjusted such that their rays touched the left and right tips (respectively) of the crack image reproduced in the EUSR GUI. Figure 8 shows a progression of cracks sizes, as they developed in specimen #2 during the fatigue testing, compared with the pictures obtained from a digital camera. The upper row of images contains the optical photos taken with a digital camera. The lower row of images contains the EUSR images of the crack obtained with the PWAS phased-array method. It is apparent that the two rows of the image show good correspondence with respect to crack length versus cycle count.

5. Power and energy transduction between PWAS and structure

The power and energy required by autonomous SHM system is of utmost importance, especially for stand-alone embedded applications. An analytical investigation of power and energy transduction between PWAS and structure during the structural health monitoring process was recently performed by Lin and Giurgiutiu [11]. This preliminary work uses an analytical approach applied to the simple model depicted in Figure 9. The study used a 1-D analytical model to capture the power and

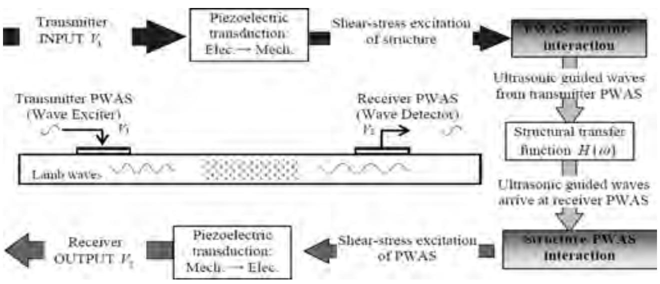

Figure 9. PWAS transmitter power and energy flow chart [11].

energy flow from the electrical source energizing the transmitter PWAS through various stages of transduction up to the signal captured by an instrument connected to the receiver PWAS.

The model consists of a transmitter PWAS (A) and a receiver PWAS (B) bonded to a metallic beam. The following energy conversion stages were considered: (a) piezoelectric transduction between source and transmitter PWAS; (b) mechanical transmission of shear stresses from the PWAS to the structure; (c) excitation of ultrasonic waves traveling through the structure from the transmitter to the receiver; (d) capturing of ultrasonic waves arriving at the receiver location; (e) mechanical conversion of structural waves into shear stresses acting from the structure onto the receiver PWAS; (f) piezoelectric conversion at the receiver PWAS and measurement by the electrical instrument.

We have developed two analytical approaches, one based on standing waves (vibration), the other based on traveling waves. The **standing-waves model** is appropriate for a finite-dimensions specimen; when excited harmonically, such a specimen will enter a state of vibration caused by the ultrasonic guided waves bouncing back and forth between the specimen boundaries in a standing-wave pattern. The **traveling-waves model** is appropriate for the study of large specimens in which the boundary effects can be neglected or for the study of wave-propagation events that happen before the waves bounce back from the reflecting boundaries. In order to account for the electronic circuit effects, considered a **voltage source** of **voltage** V_A, **source impedance** Z_A and maximum current $I_{A\max}$ and measuring instrument characterized by **instrument admittance** Y_e.

The standing-waves model is based on normal modes expansion; in the simplified case of only axial (extensional) and flexural (bending) vibrations, the voltage V_B at B is found in terms of the voltage V_A at A in the following form

$$\hat{V}_B(\omega) = \frac{k_{31}^2 Y_{0B}}{Y_e + (1-k_{31}^2)Y_{0B}} \cdot \frac{k_{iA} C_{AB}(\omega)}{N1 + N2 + N3 - 1} \hat{V}_A(\omega)$$

with

$$\begin{aligned} N1 &= R(\omega) k_{iA} k_{iB} \left[C_{AB}^2(\omega) - C_{AA}(\omega) C_{BB}(\omega) \right] \\ N2 &= k_{iA} C_{AA}(\omega) \\ N3 &= R(\omega) k_{iB} C_{BB}(\omega) \end{aligned} \quad (4)$$

where Y_{0B} is the admittance of PWAS B, k_{iA} and k_{iB} are the internal stiffnesses of PWAS A and B, k_{31} is the piezoelectric-transduction coupling factor of the PWAS material, The expressions $R(\omega)$, $C_{AA}(\omega)$, $C_{AB}(\omega)$, $C_{BB}(\omega)$ are defined in ref. [11].

The propagating-waves model assumes that axial and flexural propagating waves generated at A are felt at B and transduced into an electrical voltage which, in turn, will produce a reflected wave that will be felt back at A and will influence its ultrasonic output. Hence, the voltage V_B at B is found in terms of the voltage V_A at A in the following form

$$\hat{V}_B(\omega) = \frac{k_{31}^2 Y_{0B}}{Y_e + (1-k_{31}^2)Y_{0B}} \cdot \frac{k_{iA} C_{AB}(\omega)}{M1 - M2} \hat{V}_A(\omega)$$

with

$$\begin{aligned} M1 &= R(\omega) k_{iA} k_{iB} C_{AB}(\omega) C_{BA}(\omega) \\ M2 &= (k_{iA} C_{AA}(\omega) - 1)(R(\omega) k_{iB} C_{BB}(\omega) - 1) \end{aligned} \quad (5)$$

The coefficients $C_{AA}(\omega)$, $C_{AB}(\omega)$, $C_{AB}(\omega)$, $C_{BB}(\omega)$ are expressed in terms of propagating waves and are different than in previous equation (see ref. [11] for details). The model was used to predict the frequency response functions for voltage,

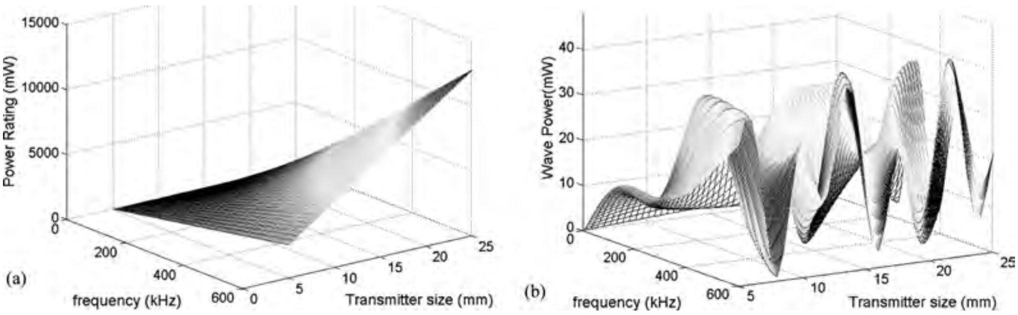

Figure 10. PWAS transmitter under constant 10-V excitation (a) power rating; (b) wave power [11].

current, complex power, active power, etc. At the input side, it was found that the reactive electric power is dominant and hence defines the size of the energizing power supply/amplifier (Figure 10a). At the PWAS structure interface, it was found that only the active electrical power gets converted into mechanical power, which is transmitted across the PWAS-structure interface and energizes the axial and flexural waves propagating into the structure. A parametric study was conducted w.r.t. the transmitter PWAS size: it was found that proper size and excitation frequency selection facilitates ultrasonic waves excitation through tuning effects. Figure 10 shows that a larger PWAS does not necessarily ensure more power transmission -- careful frequency-size tuning is necessary! Similar tuning effects were also found at the receiver PWAS where a parametric study of the receiver size, receiver impedance and external electrical load provides useful design guidelines for PWAS-based sensing and/or energy harvesting.

One-Volt three-count smoothed tone burst was applied in all cases; the results, although similar, are not identical; this highlights the challenges that need to be overcome when performing such simulations. These models need to be first subjected to validation and verification with experiments and then extended to cover multi-modal Lamb waves, various structural situations (structural variability, structural joints, flaws/damage, nonlinear friction in joints and cracks, adhesive bonding/delamination, etc.), and more complicated excitation and detection electronic circuitry.

Summary and conclusion

This paper has presented a brief introduction to structural health monitoring (SHM) with piezoelectric wafer active sensors (PWAS). A brief review of the PWAS transducers physical principles was followed by a clarification of how these novel transducers differ from the piezoelectric transducers used in conventional nondestructive evaluation (NDE). The tuning between PWAS size, operating frequency, and certain guided Lamb wave modes was presented analytically and then verified experimentally. The tuning principles was subsequently used to select low-dispersion S0 waves for a phased array application using the embedded ultrasonics structural radar (EUSR) algorithm. In a carefully conducted fatigue experiment, it was proved that permanently-attached PWAS phase-arrays can be used to perform in-situ crack growth monitoring and direct imaging of crack size under adverse noise and vibration conditions. Another important issue address in this paper is that of power and energy requirements for effective usage of PWAS transducers in active SHM applications. A theoretical model was developed for estimating the electrical power and energy required to be applied to the PWAS transducers in order to achieve a certain ultrasonic wave intensity in the test specimen. This model was used to perform a parameter study of the joint influence of PWAS size and excitation frequency on the power and energy input needed to achieve a certain wave power. It was found that the certain optimal combinations of PWAS size and excitation frequency give maximum wave power whereas other combinations results in minimum wave power values. These results are important for the optimum design of embedded SHM systems with autonomous functionality.

The results presented in this paper are preliminary and considerable additional research is required to bring them to practical fruition.

References

[1]. White, E V (2009) “Structural Health Management: System Integration Challenges and Implications,” *SMASIS 2009 ASME 2009 Conference on Smart Materials, Adaptive Structures, and Intelligent Systems*, Oxnard, CA, 2009.

[2]. Raghavan, A; Cesnik, C E S (2007) “Review of Guided-wave Structural Health Monitoring”, *Shock and Vibration Digest*, **39**(2), 91-114, 2007, doi: 10.1177/0583102406075428

[3]. Ihn, J B; Chang, F K (2008) “Pitch-catch active sensing methods in structural health monitoring for aircraft structures”, *Structural Health Monitoring - an International Journal*, **7**(1), 5-19, Mar 2008, doi: 10.1177/1475921707081979

[4]. Weaver, J; Yuan, Z; Liu, J; Collins, G; Chen, C L; Jiang, J C; He, J; Meletis, E I; Guo, R Y; Bhalla, A; Lin, B; Giurgiutiu, V; Cole, M W (2008) “Integration of Ferroelectric BaTiO3 Thin Films Directly on NiI and Ti Metallic Tapes for Structural Health Monitoring Systems and Energy Harvesting Applications”, *Integrated Ferroelectrics*, **100**, 61-71, 2008, doi: 10.1080/10584580802540355 Pii 906862671

[5]. Giurgiutiu, V, *Structural Health Monitoring with Piezoelectric Wafer Active Sensors*: Elsevier Academic Press, 2008.

[6]. Giurgiutiu, V (2005) “Tuned lamb wave excitation and detection with piezoelectric wafer active sensors for structural health monitoring”, *Journal of Intelligent Material Systems and Structures*, **16**(4), 291-305, Apr 2005, doi: Doi 10.1177/1045389x05050106

[7]. Raghavan, A; Cesnik, C E S (2005) “Finite-dimensional piezoelectric transducer modeling for guided wave based structural health monitoring”, *Smart Materials & Structures*, **14**(6), 1448-1461, Dec 2005, doi: 10.1088/0964-1726/14/6/037

[8]. Giurgiutiu, V; Bao, J; Zhao, W (2003) “Piezoelectric wafer active sensor embedded ultrasonics in beams and plates”, *Experimental Mechanics*, **43**(4), 428-449, Dec 2003

[9]. Giurgiutiu, V; Bao, J (2004) “Embedded-ultrasonics structural radar for in situ structural health monitoring of thin-wall structures”, *Structural Health Monitoring-an International Journal*, **3**(2), 121-140, Jun 2004, doi: Doi 10.1177/1475921704042697

[10]. Giurgiutiu, V; Yu, L Y; Kendall, J R; Jenkins, C (2007) “In situ imaging of crack growth with piezoelectric-wafer active sensors”, *AIAA Journal*, **45**(11), 2758-2769, Nov 2007, doi: Doi 10.2514/1-30798

[11]. Lin, B; Giurgiutiu, V (2012) “Power and energy transduction analysis of piezoelectric wafer-active sensors for structural health monitoring”, *Structural Health Monitoring - an International Journal*, **11**(1), 109-121, Jan 2012, doi: Doi 10.1177/1475921711409481